Nat Med. Author manuscript; available in PMC 2016 August 09.

Published in final edited form as:
Nat Med. 2014 June ; 20(6): 664–669. doi:10.1038/nm.3549.

Protectin DX alleviates insulin resistance by activating a myokine-liver glucoregulatory axis

Phillip J. White, **Philippe St-Pierre**, **Alexandre Charbonneau**, **Patricia Mitchell**, **Emmanuelle St-Amand**, **Bruno Marcotte**, and **André Marette**[*]
Department of Medicine, Québec Heart and Lung Institute, Université Laval, Québec, Canada

Abstract

We previously demonstrated that low biosynthesis of ω-3 derived pro-resolution mediators termed protectins is associated with an impaired global resolution capacity, inflammation and insulin resistance in obese high fat-fed mice[1]. These findings prompted a more direct study of the therapeutic potential of protectins for the treatment of metabolic disorders. Herein we found that protectin DX (PDX) exerts an unanticipated glucoregulatory activity that is distinct from its anti-inflammatory actions. PDX was found to selectively stimulate the release of the prototypic myokine interleukin-6 (IL-6) from skeletal muscle and thereby initiate a myokine-liver signaling axis, which blunts hepatic glucose production via Signal transducer and activator of transcription 3 (STAT3) mediated transcriptional suppression of the gluconeogenic program. These effects of PDX were abrogated in *IL-6* null mice. PDX also activates AMP-activated protein kinase (AMPK) but in an IL-6 independent manner. Notably, we demonstrate that administration of PDX to obese diabetic *db/db* mice raises skeletal muscle IL-6 and substantially improves insulin sensitivity in this severe model of diabetes, without any impact on adipose tissue inflammation. Our findings thus support the development of PDX-based selective muscle IL-6 secretagogues as a new class of therapy for the treatment of insulin resistance and type 2 diabetes.

Protectin DX (PDX; 10*S*,17*S*-dihydroxy-docosa-4*Z*,7*Z*,11*E*,13*Z*,15*E*,19*Z*-hexaenoic acid), is produced via sequential lipoxygenation of docosahexaenoic acid (DHA; 22:6 n-3) [2,3] and can be found alongside the first identified protectin, Protectin D1 (PD1; 10*R*,17*S*-dihydroxy-docosa-4*Z*,7*Z*,11*E*,13*E*,15*Z*,19*Z*-hexaenoic acid) in murine inflammatory exudates [2]. PDX may also be produced by human neutrophils exposed to DHA, albeit to a lesser extent than PD1 [2]. We evaluated the therapeutic potential of PDX for insulin resistance in the setting of lipid excess by employing a 6 h lipid infusion paired to a hyperinsulinemic-euglycemic clamp in lean C57BL/6J mice (Supplementary Fig. 1) [4]. We administered vehicle or PDX

[*]Correspondence: andre.marette@criucpq.ulaval.ca.

AUTHOR CONTRIBUTIONS

P.J.W. and A.M. conceived the study and wrote the manuscript. P.J.W., P.S.P., A.C., P.M. and E.S.A. performed mouse experiments. P.J.W., P.M., B.M., and E.S.A. performed cell culture experiments. P.J.W., P.M., E.S.A., and B.M. conducted ELISA and multiplex analyses, P.J.W. and P.M. carried out western blotting and PCR. All authors analyzed and discussed data and commented on the manuscript.

COMPETING FINANCIAL INTERESTS

A.M. and P.J.W. have applied for a patent describing a method and use for the stimulation of muscular IL-6 secretion.

(1μg intravenously) to lipid-infused mice immediately prior to and 2.5 h into the 6 h lipid infusion. We also clamped a saline-infused group that had been treated with vehicle to ascertain baseline insulin sensitivity. Pre-clamp glycemia was lower in PDX-treated mice compared to both vehicle-treated saline and lipid-infused animals (Fig. 1a); however, pre-clamp insulinemia was not different among groups at this time point (saline 1.4 ± 0.17 ng ml^{-1}, lipid 1.7 ± 0.09 ng ml^{-1}, lipid + PDX 1.5 ± 0.02 ng ml^{-1}; data are mean ± SEM n=6). Thus PDX appeared to possess an unanticipated insulin-independent glucoregulatory activity.

PDX-treated mice were also protected from lipid-induced insulin resistance as demonstrated by a higher glucose infusion rate (GIR) required to maintain euglycemia during the clamp compared to vehicle-treated lipid-infused mice. (Fig. 1a,b). The better insulin response in PDX-treated lipid-infused animals involved partial protection of peripheral insulin action and markedly elevated hepatic insulin action (Fig. 1c). Phosphorylation of Akt on Ser473 confirmed the stronger insulin response in skeletal muscle and liver of PDX-treated mice compared to vehicle-treated lipid-infused counterparts (Fig. 1d,e).

In line with the classical role of protectins in the active resolution of inflammation, we found that PDX also prevented lipid-mediated induction of inducible nitric oxide synthase (iNOS) in both muscle and liver (Fig. 1d,e), and c-jun n-terminal kinase (JNK) activation in liver, as determined by phosphorylation on Thr183/Tyr185 (Fig. 1e). PDX also strongly suppressed lipid-induced secretion of chemokine cc motif ligand 2 (CCL2) and 5 (CCL5) as well as tumor necrosis factor-α (TNF-α), interferon-γ (IFN-γ), interleukin-1β (IL-1β), interleukin-2 (IL-2) and interleukin-17 (IL-17) (Fig. 1f). However, in contrast to all other chemokines and cytokines tested, PDX-treated mice displayed ~7 fold higher IL-6 concentrations compared to mice that received lipid infusion alone (Fig. 1f). Although IL-6 was reported to underlie the insulin sensitizing actions of adiponectin in liver[5], we found that adiponectin does not account for these higher concentrations of IL-6 in PDX-treated mice since both vehicle and PDX-treated lipid-infused mice displayed similarly low concentrations of adiponectin in plasma compared to saline-infused animals (Supplementary Fig. 2a).

Since macrophages are important contributors to global chemokine and cytokine production we next examined whether PDX had the same influence in macrophages treated with palmitate *in vitro*. Here we observed that PDX effectively suppressed lipid-induced secretion of CCL2, CCL5, TNF-α, IL-2, and IL-10 as well as iNOS and JNK activation (Supplementary fig. 2b–d). However, rather than stimulating IL-6 release, here we found that PDX actually repressed lipid-induced IL-6 production in macrophages (Supplementary Fig. 2b). These data suggest that the higher concentration of circulating IL-6 in PDX-treated mice was likely derived from an alternate cellular source.

Given that IL-6 is well regarded as the prototypic ‘myokine’ (muscle derived cytokine)[6,7] we felt that skeletal muscle could be the site of higher IL-6 release in PDX-treated animals. Notably, we found that the profile of IL-6 in muscle closely resembled that of plasma (Fig. 2a), whereas, liver of PDX-treated mice did not contain higher IL-6 concentrations than liver from vehicle-treated mice (Supplementary Fig. 3a).

To confirm that PDX induces IL-6 expression and release from muscle in a cell autonomous fashion, we next treated cultured C2C12 myotubes with PDX. Here we observed that PDX stimulates a dose-dependant rise in IL-6 mRNA expression and accumulation in media within 2 h of administration, with the greatest dose prompting more than 2-fold higher IL-6 secretion and mRNA expression than vehicle (Fig. 2b). We also detected greater phosphorylation of AMPK at this timepoint in PDX-treated myotubes (Fig. 2c).

Brown adipose tissue was recently shown to regulate glucose homeostasis via secretion of IL-6[8]. However, although we observed IL-6 release from cultured T37i brown adipocytes in response to adrenergic stimuli (norepinephrine 1 μM) PDX did not stimulate IL-6 release from this cell type (Supplementary Fig. 3b). We also found that PDX neither stimulated or repressed IL-6 release or mRNA expression in macrophages that had not been treated with palmitate (Supplementary Fig. 3c,d). However, despite the lack of effect on IL-6 release, we found that PDX maintained its ability to promote AMPK phosphorylation (Supplementary Fig. 3e). Activation of AMPK represses inflammatory cytokine production in activated macrophages[9] and thus may underlie the PDX-mediated inhibition of IL-6 release in our earlier macrophage studies with palmitate.

To determine the structural specificity of PDX-mediated muscle IL-6 release we next assessed the potential of three structurally related lipid mediators, PD1, 8(S) 15(S) DiHETE, and Resolvin D1 (RvD1) to stimulate IL-6 production from C2C12 myotubes. These lipids were chosen because they possess a broad range of common structural features with PDX (Supplementary Fig. 3f). However, only administration of PDX prompted IL-6 release from muscle cells (Supplementary Fig. 3f). These comparative structure-function analyses thus revealed that PDX's ability to trigger IL-6 release was not solely dependent on the DHA backbone, nor based on the number, position, and stereochemistry of the hydroxyl groups alone, and cannot simply be linked to the *E, Z, E* organization of the conjugated triene within the PDX molecule. Thus skeletal muscle IL-6 release appears to be a unique characteristic of the PDX molecule rather than a shared feature of a novel lipid class. Together these data identify PDX as a structurally distinct selective skeletal muscle IL-6 secretagogue.

IL-6 is thought to regulate hepatic glucose production in liver via STAT3 mediated transcriptional suppression of the gluconeogenic genes *Peroxisome proliferator-activated receptor gamma coactivator 1-α* (*Ppargc1)*, *Phosphoenolpyruvate carboxykinase* (*Pck1*), and *Glucose-6-phosphatase* (*G6pc)* [10,11]. We observed that PDX promotes greater STAT3 phosphorylation in liver compared to vehicle-treated mice (Fig. 2d). The suppression of *Ppargc1* and *Pck1* in liver of PDX-treated mice was also greater than that observed with vehicle (Fig. 2e) and there was also improved suppression of *G6pc* in PDX-treated animals, compared to saline-infused mice (Fig. 2e). In line with a reported role for AMPK in IL-6 mediated enhancement of skeletal muscle glucose metabolism [12,13,14], PDX-treated mice also displayed higher phosphorylation of AMPK in muscle compared to their vehicle-treated counterparts (Fig. 2f).

To confirm the involvement of IL-6 in the beneficial effects of PDX we next performed a second round of paired lipid infusion hyperinsulinemic-euglycemic clamp studies in *IL-6*

null (KO) mice alongside genetically matched wild-type (WT) counterparts. Saline-infused mice treated with PDX were added to the study to ascertain whether PDX also improves glucose metabolism in insulin-sensitive animals (Supplementary Fig. 4).

As observed in the previous study, lipid-infused PDX-treated WT mice displayed lower pre-clamp glycemia compared to vehicle-treated counterparts (Fig. 3a) in the absence of any change in circulating insulin (data not shown). However, this effect of PDX was completely absent in *IL-6* KO mice (Fig. 3a). Lipid-infused *IL-6* KO mice were also refractory to the PDX-mediated enhancement of GIR (Fig. 3b) and although PDX improved both peripheral and hepatic insulin action in lipid-infused WT mice (Fig. 3c) these effects were substantially blunted in *IL-6* KO mice.

Not surprisingly PDX also failed to raise IL-6 in skeletal muscle of lipid-infused *IL-6* KO mice (Fig. 3d). Accordingly the stimulatory effect of PDX on STAT3 (Fig 3e) and suppression of *Ppargc1, Pck1* and *G6pc* (Fig. 3f) was found to be completely absent in lipid-infused *IL-6* KO mice. Systemic absence of IL-6 also lead to higher *Pck1* expression compared to vehicle treated WT mice (Fig. 3f); however, this was not the case for *G6pc* whose expression was significantly lower compared to vehicle-treated WT counterparts (Fig. 3f). This discrepant effect of IL-6 deficiency on *Pck1* and *G6Pc* expression may explain the lack of further deterioration of hepatic insulin action in lipid-infused *IL-6* KO mice.

We observed similar effects of PDX on pre-clamp glycemia, GIR and skeletal muscle IL-6 in insulin sensitive saline-infused WT mice (Supplementary Fig. 4a,b and d). However, in contrast to lipid-infused mice, the improved insulin sensitivity witnessed in the WT PDX-treated saline-infused mice was entirely the result of superior hepatic insulin action (Supplementary Fig. 4c). Of note, the IL-6 dependent activation of STAT3 by PDX was not associated with further suppression of *Ppargc1* in insulin-sensitive saline-infused mice (Supplementary Fig. 4e,f). However, PDX administration did potentiate the transcriptional repression of *Pck1* downstream of *Ppargc1* (Supplementary Fig. 4f). These effects of PDX on STAT3 and *Pck1* were found to be completely absent in saline-infused *IL-6* KO mice. PDX administration also tended to improve the suppression of *G6pc* in saline-infused WT mice (P=0.0614; Supplementary Fig. 4f) but this was not the case for *IL-6* KO counterparts. The expression of *Pck1* and *G6pc* in saline-infused *IL-6* KO mice was higher than in vehicle-treated WT mice (Supplementary Fig. 4f), which is consistent with the reduced hepatic insulin action in these mice (Supplementary Fig. 4c). It is noteworthy that PDX improved the inhibition of hepatic glucose output and suppression of gluconeogenic enzymes in these insulin sensitive saline-infused mice without potentiating Akt phosphorylation (Supplementary Fig. 5a) suggesting that the hepatic STAT3 axis is the major pathway responsible for the glucoregulatory effects of PDX.

We also found that PDX-treated *IL-6* KO mice exhibit comparable AMPK phosphorylation to WT PDX-treated mice (Fig. 3g and Supplementary Fig. 4g). In light of these data we reexamined the early timeline of PDX-mediated IL-6 release and AMPK activation in C2C12 myotubes. Here we found that PDX promotes AMPK phosphorylation within 30 minutes but no IL-6 release can be detected in the media at this time point (Supplementary Fig. 5b,c). We also found that PDX maintained its ability to potently suppress lipid-induced

elevations in circulating TNF-α in *IL-6* KO mice (Supplementary Fig. 5d). Thus our data suggest that the major glucoregulatory mechanisms of PDX are distinct from its anti-inflammatory actions and ability to activate AMPK.

We further explored the therapeutic efficacy of PDX in genetically obese *db/db* mice, a well-established model of type 2 diabetes. In these experiments, *db/db* mice were treated with vehicle or PDX (2 μg intravenously) 240 and 90 min prior to the initiation of a hyperinsulinemic-isoglycemic clamp. As observed previously, PDX tended to lower pre-clamp glycemia (Fig. 4a) but this effect did not reach statistical significance in these severely diabetic mice. Nonetheless, PDX treatment substantially improved insulin sensitivity, as revealed by a 3.6-fold higher GIR compared to vehicle-treated animals (Fig. 4b). It is noteworthy that in these obese diabetic mice the impact of PDX on GIR began to dissipate around 80 minutes into the clamp. This aligns well with a lack of enhanced STAT3 signal in liver at the completion of the clamp (Supplementary Fig. 5e) and a recent report showing that obese mice express 3-fold higher levels of 15-hydroxyprostaglandin dehydrogenase (EOR/15-PGDH) which is responsible for the enzymatic conversion of docosanoid resolution mediators to less active oxo-derivatives[15]. Nevertheless, greater suppression of STAT3 transcriptional targets, *Ppargc1*, *Pck1*, and *G6pc* was still observed in liver of PDX-treated *db/db* mice compared to vehicle-treated counterparts (Fig. 4c). Of note, these effects occurred in the absence of any significant anti-inflammatory impact of PDX on adipose tissue chemokines or cytokines (Fig. 4d). However as observed in earlier studies, PDX-treated mice exhibited higher IL-6 concentrations in skeletal muscle and plasma (Fig. 4e).

In order to determine whether the beneficial effects of PDX could be sustained or improved with a prolonged treatment regimen, we next administered 2 μg of PDX or vehicle to 17 week-old *db/db* mice twice daily for 5 days leading up to the clamp experiment. As in the acute study PDX administration tended to lower glycemia in the absence of any effect on circulating insulin (Supplementary Fig. 6a,b); however, this did not reach significance in these severely obese diabetic mice. Nonetheless the improved insulin sensitivity observed in *db/db* mice treated acutely with PDX was conserved in those mice treated with PDX for 5 days (Supplementary Fig. 6c) and once again associated with higher concentrations of skeletal muscle IL-6 and a trend for higher plasma IL-6 (Supplementary Fig. 6d). Thus the effectiveness of PDX does not appear to dissipate with extended treatment. Furthermore, lengthening the PDX treatment regimen to 5 days was not sufficient to resolve inflammatory cytokine production in adipose tissue or plasma of these very obese diabetic mice (Supplementary Fig. 6e,f). Thus the glucoregulatory axis of PDX action appears to be entirely responsible for the improved glucose utilization observed in these obese diabetic mice.

To the best of our knowledge this is the first report of an agent other than contraction/exercise that selectively promotes skeletal muscle IL-6 expression and release. The remarkable potency exhibited by PDX for the treatment of insulin resistance and type 2 diabetes suggests that skeletal muscle IL-6 secretagogues could become an exciting new class of agents for diabetes therapy. Further study of the mechanisms by which PDX promotes muscle IL-6 release is thus warranted.

This is also the first report where *IL-6* KO mice were studied using the hyperinsulinemic-euglycemic clamp in conditions of lipid excess. Although lipid infusion and palmitate treatment do increase systemic and macrophage IL-6 production, respectively, our findings do not support a role for IL-6 in the development of lipid-induced insulin resistance since we found that lack of IL-6 does not prevent insulin resistance in lipid-infused mice. To the contrary, we found that insulin-sensitive saline-infused *IL-6* KO mice display a slight defect in hepatic insulin action that is associated with altered regulation of hepatic *Pck1* and *G6pc*. Our data thus join a growing body of work [5,12,16,17] that argues for a positive role of IL-6 in the regulation of glucose metabolism.

We found that in addition to potentiating insulin action, PDX administration also induced a characteristic lowering of basal glycemia that was IL-6 dependent and preceded insulin administration in both saline and lipid-infused mice. In additional studies performed in non-clamped mice we observed that this PDX-dependent glucose lowering effect lasts for approximately 2.5 h in lean mice (data not shown). This suggests that PDX and IL-6 might also represent promising therapeutic targets as insulin-independent glucose lowering agents. This finding is in agreement with work demonstrating that exposure of mouse soleus to IL-6 and soluble IL-6 receptor increases glucose transport *ex vivo* [18] and with a study showing that the hypoglycemic response to endotoxemia is absent in *IL-6* KO mice [19]. Notably, our data suggest that the glucose lowering effect of PDX is dependent on IL-6 mediated activation of hepatic STAT3 which suppresses the expression of *Ppargc1*, *Pck1* and *G6pc*[11].

In addition to uncovering the insulin sensitizing and glucoregulatory actions of PDX, this is also the first report demonstrating that PDX can suppress lipid-induced inflammation. Although the precise mechanism underlying this anti-inflammatory activity remains to be fully defined it is plausible that activation of AMPK might underlie part of the anti-inflammatory activity of PDX [20,21]. Of note, our studies in *IL-6* KO mice revealed that PDX-dependent AMPK activation and TNF-α repression alone is not sufficient to entirely prevent the onset of lipid-induced insulin resistance. Although we cannot rule out the possibility that higher AMPK activation is required in concert with IL-6 to elicit the glucoregulatory effects of PDX we did find that PDX treatment improves insulin sensitivity in obese *db/db* mice without affecting the inflammatory phenotype of these animals. Further studies are therefore warranted in *AMPK* null animals to determine what role AMPK might play in the glucoregulatory and anti-inflammatory activities of PDX. It may also be possible that AMPK activation is necessary for PDX mediated IL-6 release.

In conclusion, our studies identify the docosanoid resolution mediator, PDX, as a novel agent that carries potent therapeutic potential for lipid-induced and obesity-linked insulin resistance and type 2 diabetes. PDX enhances both hepatic and peripheral glucose metabolism *in vivo* by promoting release of the prototypic myokine, IL-6. Notably, PDX stimulates skeletal muscle IL-6 release in a cell-specific manner that is very selective to the chemical structure of PDX. These findings may lead to the development of PDX-based muscle IL-6 secretagogues as a novel class of drugs for the treatment of insulin resistance and type 2 diabetes.

ONLINE METHODS

Animal studies

14-week old male C57BL/6J mice from Jackson Labs were used for the first paired lipid infusion hyperinsulinemic-euglycemic clamp study. These mice were placed on a standard laboratory chow diet with free access to food and water and kept in a 12h light 12h dark cycle at the Laval University hospital research centre animal facility. Mice were randomly assigned to saline, lipid or lipid + PDX groups. Five days prior to the experiment, mice were anesthetized and PE-10 catheters (Harvard Apparatus, QC, Canada) were inserted into the left common carotid artery and the right jugular vein for blood sampling and infusions respectively. Mice were fasted for 5h leading up to the protocol. Immediately prior to the start of the lipid infusion, PDX (1ug) or an equal volume of vehicle was administered via the jugular catheter to each group. Mice were then infused for 6 h with saline (5 ml kg h^{-1}) or lipid (20% intralipid emulsion (Baxter, ON, Canada) 5ml kg h^{-1} with 20 IU ml^{-1} heparin (LEO pharma, ON, Canada)). 2.5 h into the infusion PDX (1 μg) or vehicle was again administered to the appropriate groups and the HIE clamp was initiated as previously described [4,22]. The clamp protocol consisted of a 90 min tracer equilibration period followed by a 120 min experimental period. A 5 μCi bolus of [3-^{3}H] glucose was given at the start of the tracer equilibration period followed by a 0.05 μCi min^{-1} infusion for 90 min. Blood samples were drawn for the assessment of glycemia, insulin and glucose turnover levels. Following the 90 min tracer equilibration period the clamp began with a primed-continuous infusion of human insulin (16 mU kg^{-1} bolus followed by 4 mU kg min^{-1}, Humulin R; Eli Lilly, Indianapolis, IN). The [3-^{3}H] glucose infusion was increased to 0.2 μCi min^{-1} for the remainder of the experiment. Euglycemia (6.0–7.0 mM) was maintained during clamps by infusing 20% dextrose as necessary. Blood samples were taken continuously to determine glucose specific activity as well as insulin concentrations. Mice received saline-washed erythrocytes from donor mice throughout the experimental period (5–6 μl min^{-1}) to prevent a fall of ≥ 5 % hematocrit. HGP and Rd were determined using Mari's non-steady-state equations for a two-compartmental model [23].

For the second paired lipid infusion HIE clamp study, 10 week old male B6.129S2-Il6^{tmkopf}/J (*IL-6* KO) and genetically matched control (WT) mice from Jackson Labs were used. Mice from each genetic background were randomly assigned to saline-vehicle, saline-PDX, lipid-vehicle and lipid-PDX groups. The lipid-infusion clamp study was performed as described above, except the clamp was performed with a 2.5 mU kg min^{-1} insulin infusion as per [24] to ensure detection of potential differences between insulin-sensitive saline-infused animals.

The 4 mU kg^{-1} hyperinsulinemic-isoglycemic clamp study was performed in 10 week old *db/db* mice from the BKS.Cg-*Dock7*^{m} +/+ *Lepr*^{db}/J strain at Jackson Labs. Mice were randomly assigned to vehicle or PDX treatment groups. In preparation for the clamps mice were catheterized as described for the lipid infusion study. Mice were administered 2 ug of PDX or an equal volume of vehicle intravenously at 4 h and also 90 min prior to the initiation of the insulin pump. Pre-clamp glycemia was taken immediately prior to the second injection of PDX. The clamp began 90 minutes later with a primed-continuous

infusion of human insulin (16 mU kg^{-1} bolus followed by 4 mU kg min^{-1}, Humulin R; Eli Lilly, Indianapolis, IN). Glycemia was maintained as close as possible to individual fasting values by infusing 20 % dextrose as necessary. Blood samples were taken continuously to determine glycemia as well as insulin concentrations. Mice received saline-washed erythrocytes from donor mice throughout the experimental period (5–6 μl min^{-1}) to prevent a fall of ≥ 5 % hematocrit. The chronic PDX experiments were performed as described for the acute study except that PDX was administered twice daily at a dose of 2 μg intravenously, and for 5 consecutive days until the day of the clamp. On clamp day the protocol was performed precisely as described above for the acute study.

All animal procedures were approved and carried out in accordance with directions of The Laval University Council for Animal Care and Canadian Council for Animal Care.

C2C12 myotubes

C2C12 myoblasts were maintained in DMEM containing 10% FBS. Differentiation to myotubes was initiated by addition of DMEM containing 2% horse serum. The experiment was conducted 5 days after the addition of the differentiation media. Immediately prior to the commencement of experiments fresh media was added to the cells. Then vehicle or PDX (10, 100 nM, and 1 μg) was added to the appropriate wells. 30 and 120 min after the addition of PDX media was collected and frozen for IL-6 quantification and cells were washed in ice cold PBS. For extraction of mRNA, cells were then lysed and scraped in 300μl of RLT buffer (QIAGEN). For examination of AMPK activity cells were lysed and scraped in 200 μl of ice cold lysis buffer containing 50 mM HEPES pH7.5, 150 mM NaCl, 1 mM EGTA, 20 mM b-glycerophosphate, 1 % NP40, 10 mM NaF, 2 mM Na3VO4, 1x protease inhibitor cocktail (Sigma). For structure function studies we compared the activity of PDX (100nM) with 100nM of PD1, RvD1 (Cayman chemical), or 8(S)15(S)DiHETE (Cayman chemical). After 2 h of incubation with these lipid mediators media was collected and IL-6 determined as described above.

Macrophages

J774A.1 murine macrophages (ATCC) were maintained in DMEM (10 % FBS) until 80 % confluence. For palmitate stimulation studies a 2 mM palmitate solution or methanol vehicle in alpha-MEM (12 % BSA) was added to fresh DMEM (10 % FBS) to give a final concentration of 400 μM palmitate. Concomitantly, PDX (10 or 100 nM, Cayman chemical), or vehicle was added to the media. After 16 h, the media was collected and cells were lysed as described for the studies in C2C12 mytoubes. For IL-6 release studies fresh DMEM (10 % FBS) was added to the cells and they were stimulated with PDX (Cayman chemical), vehicle, or LPS (100 ng mL^{-1}) the media was collected and cells were lysed as described above.

Brown Adipocytes

T37i fibroblasts were cultured in DMEM/HamF12 (Gibco-Invitrogen) supplemented with 10 % FBS, 100IU ml^{-1} penicillin, 100 g ml^{-1} streptomycin, and 20 mM HEPES and grown at 37 °C in a humidified atmosphere with 5 % CO_2. Differentiation into brown adipocytes was achieved under standard conditions by incubation of subconfluent T37i cells with 2 nM

triiodothyronine and 20 nM insulin for at least 7 days. Experiments were performed 7 days post differentiation. On the day of the experiment media was replaced and cells were stimulated with 100 nM PDX (Cayman chemical), vehicle, or norepinephrine (Sigma), and the media was collected and IL-6 determined as described above.

Western blotting

Snap frozen gastrocnemius muscle and liver from mice were pulverized in liquid nitrogen then lysed overnight at 4 °C in the lysis buffer described for the C2C12 myotube experiments. Immunoblotting of myotube, macrophage, liver and muscle lysates was then performed as previously described [1]. Briefly, 50μg of protein was loaded onto a 7.5 % acrylamide gel, subjected to SDS-PAGE then transferred onto nitrocellulose membranes. Membranes were cut into molecular weight regions containing the protein of interest (Akt 52–76 Kda; JNK and AMPK 38–76 Kda; STAT3 76–102 Kda; iNOS 102–150 Kda) then blocked and probed with the appropriate antibodies. All primary antibodies were used at a concentration of 1:1,000. Secondary antibodies were diluted 1:10,000. Antibodies for p-Akt ser473 (CST9271) [1,25], p-JNK Thr183/Tyr185 (CST9251) [1,26], JNK (CST9252) [1,26], p-AMPK Thr172 (CST2535) [21,27], AMPK (CST2532) [21,27], p-STAT3 Ser727 (CST9134) [28,29] and STAT3 (CST9132) [28,29] were obtained from Cell Signaling Technology (MA, USA). Antibodies for total Akt (sc-8312) [1,25] and iNOS (#610330) [1,21] were from Santa Cruz Biotechnology (CA, USA) and BD Transduction Laboratories™ (Canada) respectively.

Real-time RT-PCR

RNA was extracted from C2C12 myotubes using an RNeasy® mini kit from QIAGEN. RNA from homogenized liver tissue was extracted using an RNeasy® fibrous tissue mini kit from QIAGEN. RNA was then reverse transcribed to cDNA using the high-capacity cDNA reverse transcription kit from applied biosystems. Real-time PCR for *Ppargc1*, *Pck1*, *G6Pc*, and *Gapdh* was then performed using Taqman assay on demand probes and primers from Applied Biosystems in a CFX96 real-time system from BIO-RAD. The relative expression of genes of interest was then determined by normalization to the reference gene GAPDH using the comparative C_T method for relative gene expression [30].

Analytical methods

Chemokines and cytokines were quantified in macrophage media, or mouse plasma using the MILLIPLEX™ MAP mouse cytokine/chemokine kit (Millipore Corporation, MA, USA). Nitrite accumulation in media was determined by Greiss assay as previously described [20]. Plasma insulin levels were assessed by RIA (Linco, MI, USA). FFA were measured using an enzymatic colorimetric assay (Wako Chemicals, VA, USA). IL-6 was quantified in mouse skeletal muscle and liver as well as C2C12, T37i, and non-stimulated macrophages using the mouse IL-6 ELISA kit from R&D systems. Total plasma adiponectin was determined using the ELISA from ALPCO.

Statistical Analysis

An unpaired Student's t-test was used to identify statistically significant differences between two groups. For comparison among more than two groups a one-way analysis of variance

was used followed by Newman-Keuls multiple comparison test. P-values of <0.05 were considered significant.

Supplementary Material

Refer to Web version on PubMed Central for supplementary material.

Acknowledgments

We would like to thank C. Dion for surgical preparation of the mice and S. Pelletier for his assistance with the palmitate macrophage studies. We also thank C. Serhan (Brigham and Women's Hospital, Harvard) and N. Flamand (Heart and Lung Institute, Laval University) for the kind gifts of PD1 and 8(S)15(S)DiHETE respectively, and M. Schwab and K. Bellmann for their help with the PCR analyses. T37i fibroblasts were a generous gift from M. Lombès, INSERM U478, Paris, France. This work was supported by grants to A.M. from the Canadian Diabetes Association and from the Canadian Institutes of Health Research (CIHR). A.M. is the holder of a CIHR/Pfizer research Chair in the pathogenesis of insulin resistance and cardiovascular diseases. P.J.W. is the recipient of a PhD studentship from the Fonds de la Recherche en Santé du Quebec.

References

1. White PJ, Arita M, Taguchi R, Kang JX, Marette A. Transgenic restoration of long-chain n-3 fatty acids in insulin target tissues improves resolution capacity and alleviates obesity-linked inflammation and insulin resistance in high-fat-fed mice. Diabetes. 2010; 59:3066–3073. [PubMed: 20841610]
2. Serhan CN, et al. Anti-inflammatory actions of neuroprotectin D1/protectin D1 and its natural stereoisomers: assignments of dihydroxy-containing docosatrienes. J Immunol. 2006; 176:1848–1859. [PubMed: 16424216]
3. Chen P, et al. Full characterization of PDX, a neuroprotectin/protectin D1 isomer, which inhibits blood platelet aggregation. FEBS Lett. 2009; 583:3478–3484. [PubMed: 19818771]
4. Charbonneau A, Marette A. Inducible nitric oxide synthase induction underlies lipid-induced hepatic insulin resistance in mice: potential role of tyrosine nitration of insulin signaling proteins. Diabetes. 2010; 59:861–871. [PubMed: 20103705]
5. Awazawa M, et al. Adiponectin enhances insulin sensitivity by increasing hepatic IRS-2 expression via a macrophage-derived IL-6-dependent pathway. Cell Metab. 2011; 13:401–412. [PubMed: 21459325]
6. Pedersen BK, Febbraio MA. Muscle as an endocrine organ: focus on muscle-derived interleukin-6. Physiological reviews. 2008; 88:1379–1406. [PubMed: 18923185]
7. Pedersen BK, Febbraio MA. Muscles, exercise and obesity: skeletal muscle as a secretory organ. Nature reviews. Endocrinology. 2012
8. Stanford KI, et al. Brown adipose tissue regulates glucose homeostasis and insulin sensitivity. J Clin Invest. 2013; 123:215–223. [PubMed: 23221344]
9. Sag D, Carling D, Stout RD, Suttles J. Adenosine 5′-monophosphate-activated protein kinase promotes macrophage polarization to an anti-inflammatory functional phenotype. J Immunol. 2008; 181:8633–8641. [PubMed: 19050283]
10. Inoue H, et al. Role of hepatic STAT3 in brain-insulin action on hepatic glucose production. Cell Metab. 2006; 3:267–275. [PubMed: 16581004]
11. Inoue H, et al. Role of STAT-3 in regulation of hepatic gluconeogenic genes and carbohydrate metabolism in vivo. Nat Med. 2004; 10:168–174. [PubMed: 14716305]
12. Carey AL, et al. Interleukin-6 increases insulin-stimulated glucose disposal in humans and glucose uptake and fatty acid oxidation in vitro via AMP-activated protein kinase. Diabetes. 2006; 55:2688–2697. [PubMed: 17003332]
13. Kelly M, Gauthier MS, Saha AK, Ruderman NB. Activation of AMP-activated protein kinase by interleukin-6 in rat skeletal muscle: association with changes in cAMP, energy state, and endogenous fuel mobilization. Diabetes. 2009; 58:1953–1960. [PubMed: 19502419]

14. Kelly M, et al. AMPK activity is diminished in tissues of IL-6 knockout mice: the effect of exercise. Biochem Biophys Res Commun. 2004; 320:449–454. [PubMed: 15219849]
15. Claria J, Dalli J, Yacoubian S, Gao F, Serhan CN. Resolvin D1 and resolvin D2 govern local inflammatory tone in obese fat. J Immunol. 2012; 189:2597–2605. [PubMed: 22844113]
16. Wunderlich FT, et al. Interleukin-6 signaling in liver-parenchymal cells suppresses hepatic inflammation and improves systemic insulin action. Cell Metab. 2010; 12:237–249. [PubMed: 20816090]
17. Pedersen BK, Febbraio MA. Point: Interleukin-6 does have a beneficial role in insulin sensitivity and glucose homeostasis. J Appl Physiol. 2007; 102:814–816. [PubMed: 17068210]
18. Gray SR, Ratkevicius A, Wackerhage H, Coats P, Nimmo MA. The effect of interleukin-6 and the interleukin-6 receptor on glucose transport in mouse skeletal muscle. Exp Physiol. 2009; 94:899–905. [PubMed: 19482899]
19. Tweedell A, et al. Metabolic response to endotoxin in vivo in the conscious mouse: role of interleukin-6. Metabolism. 2011; 60:92–98. [PubMed: 20102773]
20. Pilon G, Dallaire P, Marette A. Inhibition of inducible nitric-oxide synthase by activators of AMP-activated protein kinase: a new mechanism of action of insulin-sensitizing drugs. J Biol Chem. 2004; 279:20767–20774. [PubMed: 14985344]
21. Centeno-Baez C, Dallaire P, Marette A. Resveratrol inhibition of inducible nitric oxide synthase in skeletal muscle involves AMPK but not SIRT1. Am J Physiol Endocrinol Metab. 2011; 301:E922–930. [PubMed: 21810931]
22. Xu E, et al. Targeted disruption of carcinoembryonic antigen-related cell adhesion molecule 1 promotes diet-induced hepatic steatosis and insulin resistance. Endocrinology. 2009; 150:3503–3512. [PubMed: 19406938]
23. Mari A. Estimation of the rate of appearance in the non-steady state with a two-compartment model. Am J Physiol. 1992; 263:E400–415. [PubMed: 1514623]
24. Mulvihill EE, et al. Nobiletin attenuates VLDL overproduction, dyslipidemia, and atherosclerosis in mice with diet-induced insulin resistance. Diabetes. 2011; 60:1446–1457. [PubMed: 21471511]
25. Xu E, et al. Hepatocyte-specific Ptpn6 deletion protects from obesity-linked hepatic insulin resistance. Diabetes. 2012; 61:1949–1958. [PubMed: 22698917]
26. Chung J, et al. HSP72 protects against obesity-induced insulin resistance. Proc Natl Acad Sci U S A. 2008; 105:1739–1744. [PubMed: 18223156]
27. Jenkins Y, et al. AMPK activation through mitochondrial regulation results in increased substrate oxidation and improved metabolic parameters in models of diabetes. PLoS One. 2013; 8:e81870. [PubMed: 24339975]
28. Moh A, et al. STAT3 sensitizes insulin signaling by negatively regulating glycogen synthase kinase-3 beta. Diabetes. 2008; 57:1227–1235. [PubMed: 18268048]
29. Rio A, et al. Reduced liver injury in the interleukin-6 knockout mice by chronic carbon tetrachloride administration. Eur J Clin Invest. 2008; 38:306–316. [PubMed: 18371088]
30. Schmittgen TD, Livak KJ. Analyzing real-time PCR data by the comparative C(T) method. Nat Protoc. 2008; 3:1101–1108. [PubMed: 18546601]

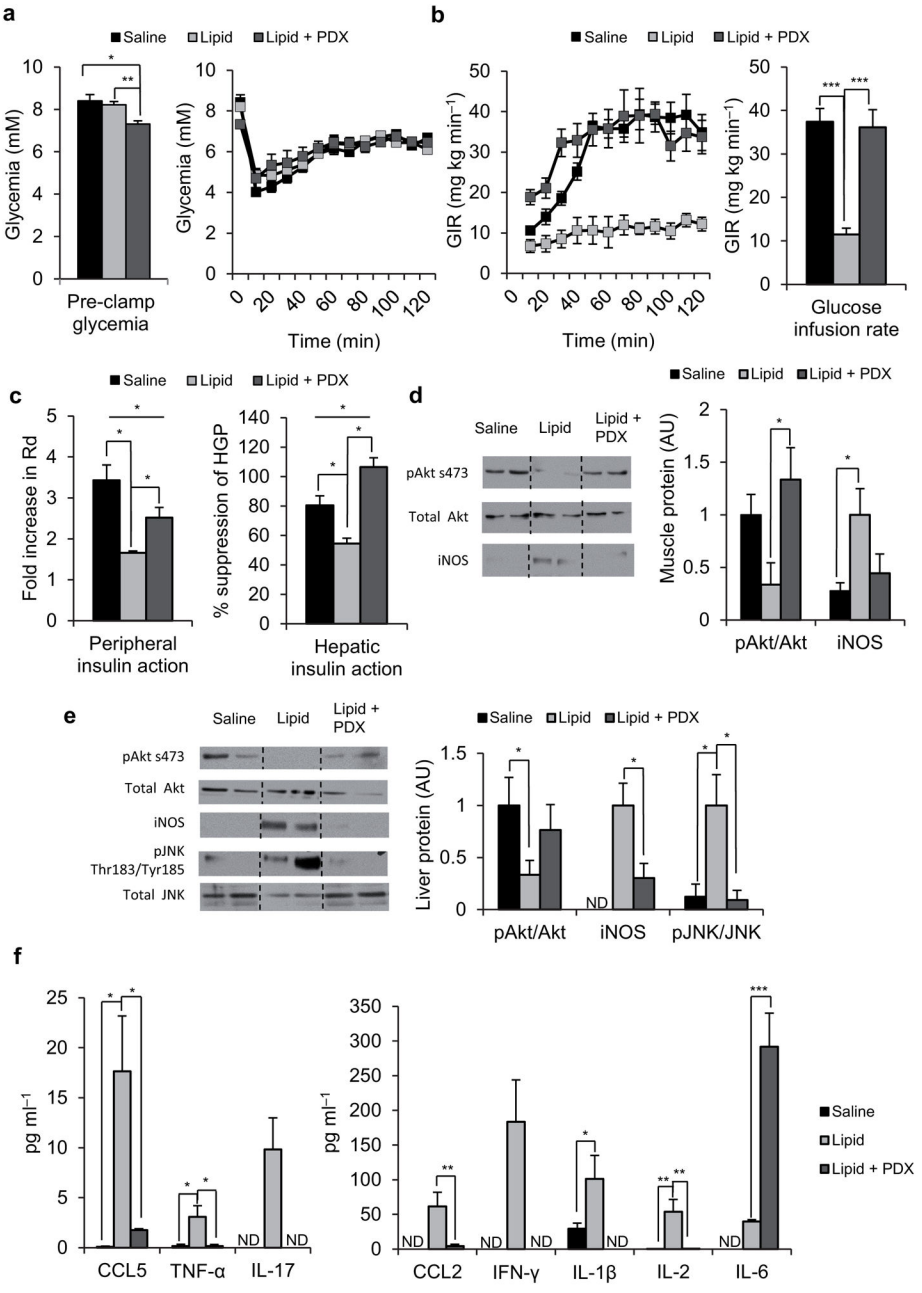

Figure 1.

PDX prevents lipid-induced insulin resistance. **(a)** Pre-clamp glycemia (left) and clamp glucose excursion (right), **(b)** glucose infusion rate (GIR) (left) and mean GIR for the final 60 min of clamp (right), **(c)** peripheral insulin action expressed as fold increase in Rd during the clamp (left) and hepatic insulin action expressed as percent suppression of hepatic glucose production (HGP; right) in saline-vehicle, lipid-vehicle and lipid-PDX treated mice **(d)** Immunoblots for pAkt ser473, total Akt and iNOS in gastrocnemius muscle of clamped saline-vehicle, lipid-vehicle and lipid-PDX treated mice. **(e)** Immunoblots for pAkt ser473, total Akt, iNOS, pJNK Thr183/Tyr185, and total JNK in liver of clamped saline-vehicle,

lipid-vehicle and lipid-PDX treated mice. Quantification of densitometry analyses are shown to the right of the representative gels. Dotted lines indicate that lanes were run on the same gel but were noncontiguous. **(f)** Chemokines and cytokines in plasma from clamped saline-vehicle, lipid-vehicle and lipid-PDX treated mice. Data are mean ± s.e.m, and are representative of 6 mice per group. AU, arbitrary units. ND, not detected, * $P<0.05$, ** $P<0.01$, *** $P<0.001$ calculated using analysis of variance.

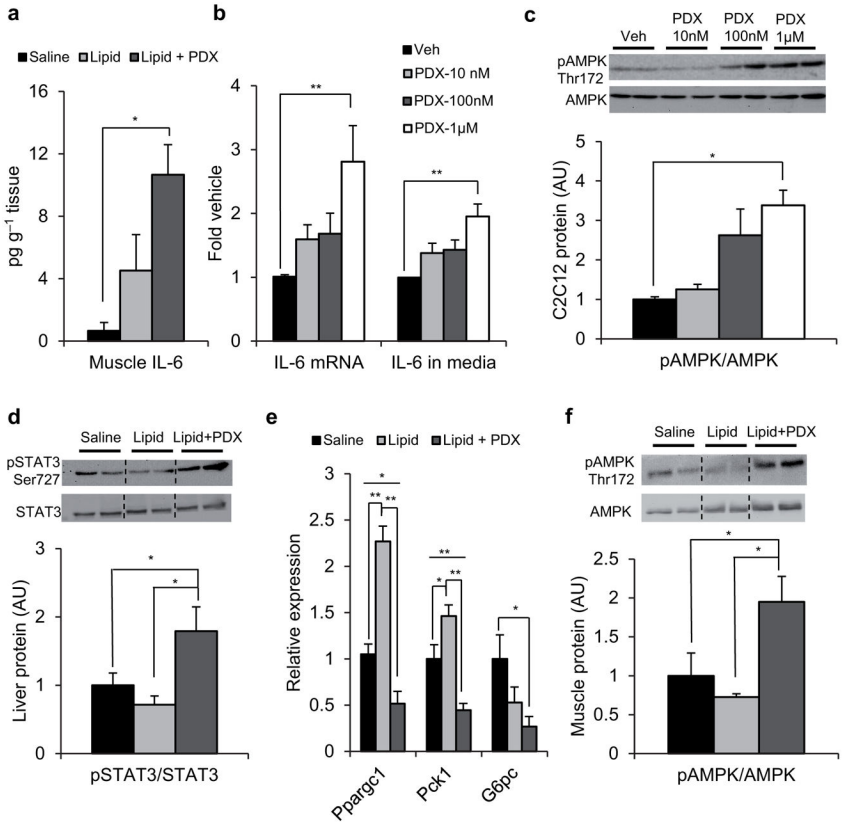

Figure 2.

PDX stimulates skeletal muscle IL-6 expression. **(a)** Skeletal muscle IL-6 protein expression in gastrocnemius from clamped saline-vehicle, lipid-vehicle and lipid-PDX treated mice. Data are mean ± s.e.m., and are representative of 6 mice per group **(b)** Fold *IL-6* mRNA expression normalized to *GAPDH* (left) and IL-6 protein secretion in media (right) and **(c)** immunoblots for pAMPK Thr172 and total AMPK in 2h PDX-treated C2C12 myotubes compared to veh control. Quantification of densitometry analyses for immunoblots is shown below the representative gels. Data are mean ± s.e.m. for three independent experiments **(d)** Immunoblots for pSTAT3 Ser727 and total STAT3 and **(e)** relative mRNA expression of *Ppargc1, Pck1 and G6Pc* normalized to *GAPDH* in liver from clamped saline-vehicle (n = 6), lipid-vehicle (n = 6) and lipid-PDX treated mice (n = 6). **(f)** Immunoblots for pAMPK Thr172 and total AMPK in gastrocnemius muscle from clamped saline-vehicle (n = 6), lipid-vehicle (n = 4) and lipid-PDX (n = 5) treated mice. Quantification of densitometry analyses for immunoblots is shown below the representative gels. Dotted lines indicate that lanes were run on the same gel but were noncontiguous. Data are mean ± s.e.m, * P<0.05, ** P<0.01 calculated using analysis of variance.

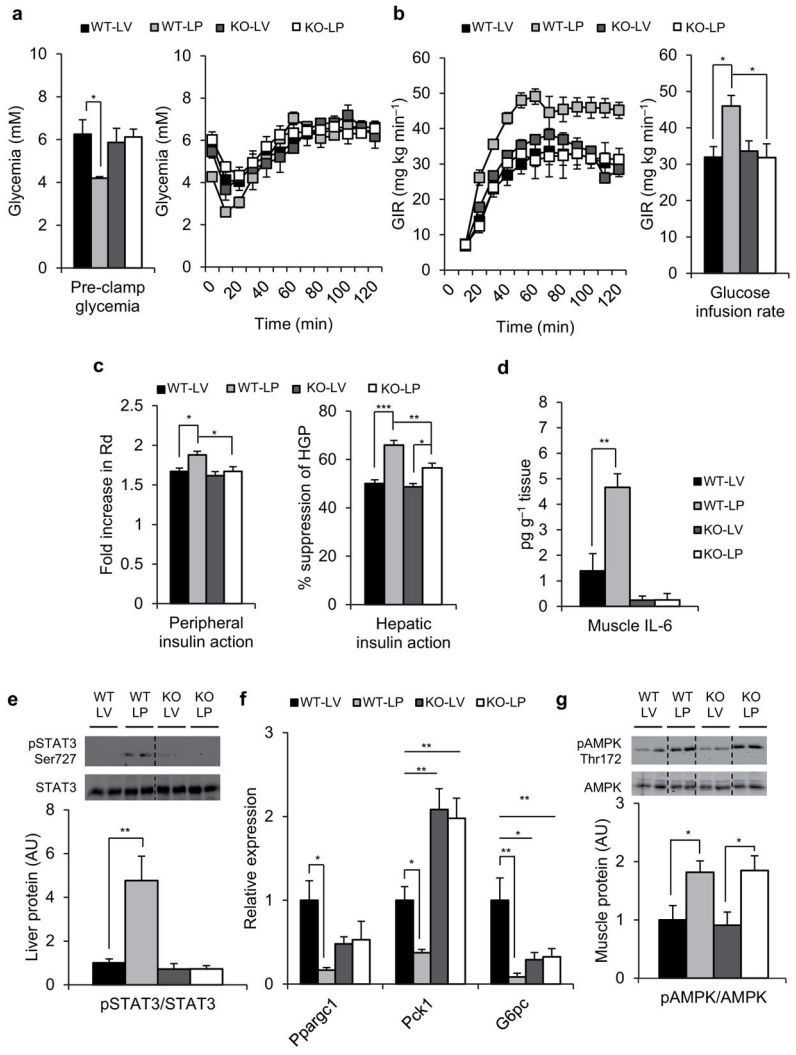

Figure 3.

IL-6 is required for the insulin sensitizing actions of PDX. **(a)** Pre-clamp glycemia (left) and clamp glucose excursion (right), **(b)** glucose infusion rate (GIR) (left) and mean GIR for the final 60 min of clamp (right) in wild-type (WT) or *IL-6* null (KO) lipid-infused (L) PDX (P) or vehicle (V) treated animals. **(c)** Peripheral insulin action expressed as fold increase in Rd during the clamp (left) and hepatic insulin action expressed as percent suppression of hepatic glucose production (HGP; right), **(d)** Skeletal muscle IL-6 content **(e)** Immunoblots for pSTAT3 Ser727 and total STAT3 and **(f)** relative mRNA expression of *Ppargc1, Pck1 and G6Pc* normalized to *GAPDH* in liver from clamped wild-type (WT) or *IL-6* null (KO) lipid-infused (L) PDX (P) or vehicle (V) treated animals. **(g)** Immunoblots for pAMPK Thr172 and total AMPK in gastrocnemius muscle from clamped wild-type (WT) or *IL-6* null (KO) lipid-infused (L) PDX (P) or vehicle (V) treated animals. Quantification of densitometry analyses for immunoblots is shown below the representative gels. Dotted lines indicate that lanes were run on the same gel but were noncontiguous. WT-LV, wild-type lipid-infused vehicle, $n = 6$ mice. WT-LP, wild-type lipid-infused PDX, $n = 5$ mice. KO-LV, IL-6 null

lipid-infused vehicle, n = 5 mice. KO-LP, IL-6 null lipid-infused PDX, n=6 mice. Data are mean ± s.e.m, * P<0.05, **P<0.01, ***P<0.001 calculated using analysis of variance.

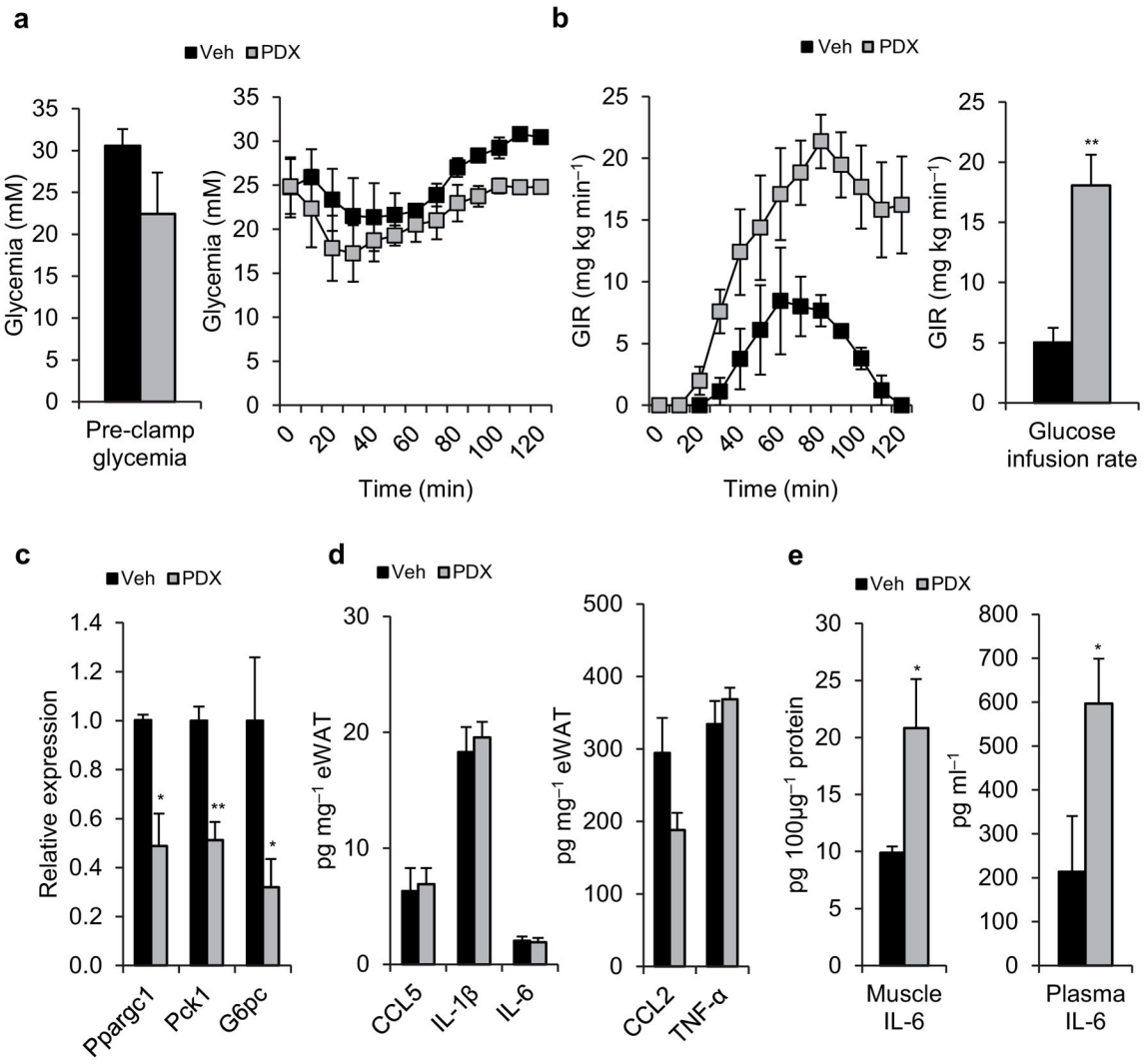

Figure 4.

PDX therapy improves insulin sensitivity in diabetic mice. **(a)** Pre-clamp glycemia (left) and clamp glucose excursion (right), **(b)** glucose infusion rate (GIR) (left) and mean GIR for the final 60 min of clamp (right) in vehicle (veh) and acute PDX-treated genetically obese diabetic *db/db* mice. **(c)** Relative mRNA expression of *Ppargc1, Pck1 and G6Pc* normalized to *GAPDH* in liver from clamped veh and acute PDX-treated *db/db* mice. **(d)** Chemokines and cytokines in epididymal white adipose tissue (eWAT) of clamped veh and acute PDX-treated *db/db* mice. **(e)** Skeletal muscle (left) and plasma (right) IL-6 content from of clamped veh and acute PDX-treated *db/db* mice. Data are mean ± s.e.m. Veh $n = 3$, PDX $n = 4$, * P<0.05, **P<0.01 calculated using Student's t-test.